Verification of a Multizone Airflow and Energy Network Model by Analytical Solutions to Stack-driven Flows in Buildings

Dahai Qi Liangzhu (Leon) Wang Radu Zmeureanu
Department of Building, Civil and Environmental Engineering, Concordia University, Montreal, Canada

Abstract

The multizone network models without energy equation are widely used to study natural ventilation, indoor air quality and smoke movement in buildings. When energy equation is included in the multizone network model, it is necessary to be verified. This study aims to verify a multizone airflow and energy network model, CONTAM97R, by analytical solutions. Solutions to a naturally ventilated single-zone room and a high-rise building with a vertical shaft under fires are employed to verify CONTAM97R. Floor Zoning Strategy (FZS) and Adaptive Zoning Strategy (AZS), are proposed and compared in an example of a sixteen-storey building. The results show that the accuracy of FZS is influenced by temperature attenuation coefficient, α. A larger α value causes more simulation error. The accuracy of FZS can be improved by increasing the total number of zones used for the shaft. Compared with FZS, AZS can obtain results with similar accuracy with less number of zones.

1 Introduction

Many of current multizone network models are often used to calculate the airflows and contaminant concentrations between different spaces (e.g. rooms) in a building, as well as between the building and the outdoors (Wang & Chen 2008). In a multizone network model, each space is defined as one zone, where the air is assumed well mixed so the associated physical parameters, e.g. air temperatures and chemical species concentrations, are spatially uniform (Chen 2009). The well-mixed assumption avoids the computing cost necessary for detailed results on finer spatial scales, and thus ensures a fast calculation on a PC: only a few seconds needed even for a whole-building airflow analysis. The simple and yet powerful capabilities of multizone network models attract many applications including indoor air quality analysis (IAQ), ventilation design, building safety and security analysis, e.g. fire smoke movement in buildings (Wang et al. 2013). Among these multizone models, CONTAM is one of the most popular models, which has been applied to many building types (Ng et al. 2012). A recent study by Ng et al. (2012 & 2013) used CONTAM for modeling the airflow and IAQ in different DOE (the US Department of Energy) reference buildings, including restaurants, offices, schools, stores, hotels, hospitals and apartments. CONTAM was also frequently used to study the smoke control strategies in buildings. Miller et al. (2009 & 2011) employed CONTAM to study the elevator shaft and stairwell shaft-pressurization system in a thirty-storey residential and a commercial building. It was found that there exist strong interactions between the stairwell and elevator shaft pressurization systems, and the fan for smoke controls should be chosen carefully.

However, CONTAM does not solve the energy conservation equation so the temperature in each zone has to be known beforehand and provided as an input from users, because it was originally developed without the intent for temperature predictions. With the many more usages of CONTAM to different building types and various practical problems, the limita-

tions due to the lack of the energy equation has started to become apparent and hinder its wider applications. Many current applications ask for the solutions to the coupled thermal airflow problems, e.g. during the designs of natural ventilations or smoke control systems in high-rise building, where the airflow is mostly driven by stack effects. Wang et al. (2013) simulated a forty-storey high-rise building during fires with CONTAM by assuming different profiles of gas temperature in the vertical shafts. The results showed that an inaccurate estimation of temperature profile could lead to an error of about 80% for the prediction of the shaft mass flow rates. Therefore, the addition of the energy analysis capability to CONTAM has become quite necessary, if it is used to solve coupled thermal airflow problems in buildings.

There have been quite a few studies to add the capability of thermal analysis to CONTAM (Tan 2005, Tan & Glicksman 2005, McDowell et al. 2003, and Gu 2011), many of which have not yet resulted in a final product. Luckily, there has already existed a version of CONTAM with the energy equation added, CONTAM97R (Axley 2011, Wang 2012). The version was firstly developed in 1997 but never publically released due to various reasons. With the mounting calls for a multizone model with the energy equation, it is time to verify how the model can be used to solve the current coupled thermal airflow problems in buildings. Some previous studies tried to evaluate the performance of CONTAM97R through experimental validations. Axley et al. (2002) compared the measured air flow rates in a naturally ventilated building to the predictions, and found that the difference could be over 25%. Such difference is also commonly seen in other experimental validation studies with a discrepancy ranging between 25% and 50% (Mahdavi & Proglhof 2008, Haghighat & Li 2004). Although experimental validation is an effective way to prove the validity of a numerical model, it is difficult to explain and isolate the causes for the discrepancies, once observed, of the measurements and the predictions. Apparently, it is not reasonable to attribute all the discrepancies to the computer model itself because there are many other contributing factors, e.g. measurement uncertainties, user inputs, simplifications and assumptions for the creation of the physical model of the problems. Therefore, experimental validation is somehow limited during the evaluation of the mathematical formulation and the numerical discretization of a computer model. In comparison, an analytical model provides a mathematical solution to the same set of conservation equations formulated in a numerical model. Therefore, a verification study based on analytical solutions is often conducted to evaluate the accuracy of a computer model (Oberkampf & Trucano 2002, McDermott et al. 2010). The analytical solutions can also help to answer for the causes for their discrepancies with the numerical model, and to suggest necessary remedies.

An exhaustive literature search shows that there have been few verification studies of the multizone network models by analytical solutions, probably due to the models themselves already being simple enough and/or a lack of available analytical solutions. This paper aims to verify the multizone airflow and energy network model, CONTAM97R, for the two current major applications of such a model: a naturally ventilated single-zone room and a high-rise building with a vertical shaft under fires. We first briefly introduce the energy model in CONTAM97R. Then, the simulation results by the computer model are compared to the analytical solution of airflows induced by stack effect and air temperatures in the single zone room (Yam et al. 2003). We then use the model to simulate the smoke dispersion in a 16-storey high-rise building with a vertical shaft. The simulation results are compared to the analytical models that we recently developed (Qi et al. 2014). We also discuss different strategies to divide the shaft into multiple sub-zones, and their impacts on the accuracy of the simulation results. When major discrepancies are observed, we try to analyze the causes for the difference and provide the suggestion on how to correctly model the shaft in the high-rise building by CONTAM97R.

2 Energy model in multizone model

The energy equation in CONTAM97R can be explained by the case in Figure 1, where zone *i* is a single room surrounded by the ambient zone, zone *j*. The air is assumed to be well mixed and static. The energy conservation equation for zone *i* can be written as:

$$\frac{d\left(C_{pi}T_i m_i\right)}{dt} = \sum_j C_{pj}T_j \dot{m}_{ji} - \sum_j C_{pi}T_i \dot{m}_{ij} + E_i + \sum_k h_{wk}\left(T_{wki} - T_i\right) \tag{1}$$

In Figure 1, zone *j* is the only neighbor zone but it can be any other zones/rooms connected directly to zone *i*. The convective heat transfer coefficient, h_{wk}, is determined by the temperature difference between the wall surface and the ambient air. The conductive heat transfer from surface thermal node *ki* to *kj* of the wall *k* is considered by Eq. (2), which is solved by the 1-D discrete method.

$$q = -k\frac{dT}{dy} \tag{2}$$

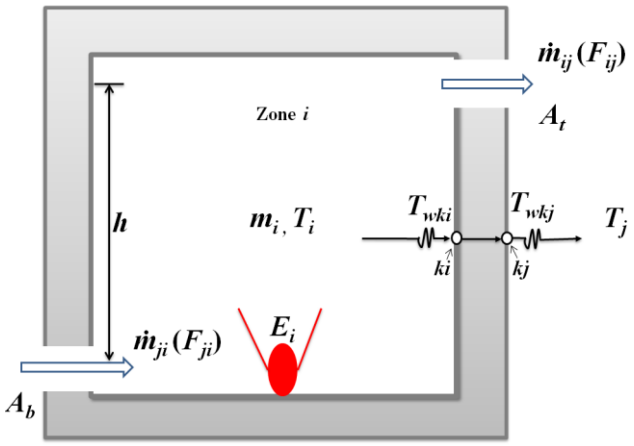

Figure 1: Schematic of the energy modeling in CONTAM97R

3 Natural ventilation in a single-zone room

Analytical model

To verify the energy model, we first use a case of natural ventilation in a single zone room from the literature (Yam et al. 2003). Yam et al. developed the analytical solutions to a series of flows induced by stack effect in the single-zone space. Their models are among those limited studies with a simple setup and clear formulations, so we choose it as the first verification case. The analytical models are based on the following assumptions: (1) air temperature distribution in the room is uniform; (2) walls are perfectly insulated; (3) thermal radiations are neglected; (4) outdoor air temperature follows a cyclic sinusoidal curve as Eq. (3) shows.

The single zone room model can refer to Figure 1 but there is no heat transfer through walls as the assumptions indicate. Eq. (1) applied to the single zone case and with the ambient temperature defined by Eq. (3) leads to Eq. (4). The ventilation flow rate equation of the single room can be written as Eq. (5) (Yam et al. 2003), where $A^* = A_t A_b / \sqrt{A_t^2 + A_b^2}$ is the effective area, and *h* is the vertical distance between the top and bottom openings (see Figure 1). We then define thermal mass number, φ, in Eq. (6), which is the ratio between the maximum heat stored $mC_p\omega\Delta\tilde{T}_o$ by indoor air and the total heat gain, *E*, in the building (Yam et al. 2003). When φ to be infinite, indoor temperature, T_i, becomes constant and the volume flow

rate, F, is only influenced by the fluctuation of the outdoor temperature T_o. So there exist analytical solutions for F and T_i, as Eqs. (7) and (8) show.

$$T_o = \tilde{T}_o + \Delta\tilde{T}_o \sin(\omega t) \tag{3}$$

$$\omega m C_p \frac{d(T_i)}{d(\omega t)} + \rho C_p |F|(T_i - T_o) = E \tag{4}$$

$$F|F| = (C_d A^*)^2 2gh(T_i - T_o)/\tilde{T}_o \tag{5}$$

$$\varphi = mC_p \omega \Delta\tilde{T}_o / E \tag{6}$$

$$|F|F = -\frac{2\eta^3}{\lambda}\sin(\omega t) + C \tag{7}$$

$$T_i(\omega t) = \left[1 + \frac{C}{2gh(C_d A^*)^2}\right]\tilde{T}_o \tag{8}$$

where

$$\eta = (C_d A^*)^{2/3}(Bh)^{1/3} \tag{8}$$

$$B = \frac{Eg}{\rho C_P \Delta\tilde{T}_o} \tag{9}$$

$$\lambda = \frac{E}{\rho C_P \Delta\tilde{T}_o} \tag{10}$$

Simulations and verifications

To match the conditions in the analytical solutions, we set up the CONTAM97R simulations by using the parameters in Table 1. Since in CONTAM97R, φ cannot be infinite, we choose a very large value of φ (φ=7×10^6) to approximate infinity. Walls are insulated, and the time step is 10 minutes.

Table 1: Calculation parameters

Parameter	A^* (m^2)	$\tilde{T}_o$ (K)	$\Delta\tilde{T}_o$ (K)	h (m)	C_d	η (m^3/s)	B (m^4/s^3)	λ (m^3/s)	φ	ω
Values	0.707	300	8	19	0.6	0.04545	2.72×10^{-5}	1×10^{-4}	7×10^6	*π/12*

Figure 2 shows the simulation results for the time period of 696 ~ 744 hours (48 hours), when the ventilation flow and indoor temperature is periodically steady. We choose the air flow rate at the time of 696 hour, which is -0.284 m^3/s, as the initial condition to get the constant C in Eq. (7). Similar plots can be obtained for the air flow rates selected at other times. Figure 2 shows that the simulation results are very close to the analytical solutions. The average relative difference of air flow rate is about 1.6%, which might be caused by the difference between the simulation finite value of φ and the infinite value of φ used in the analytical solution.

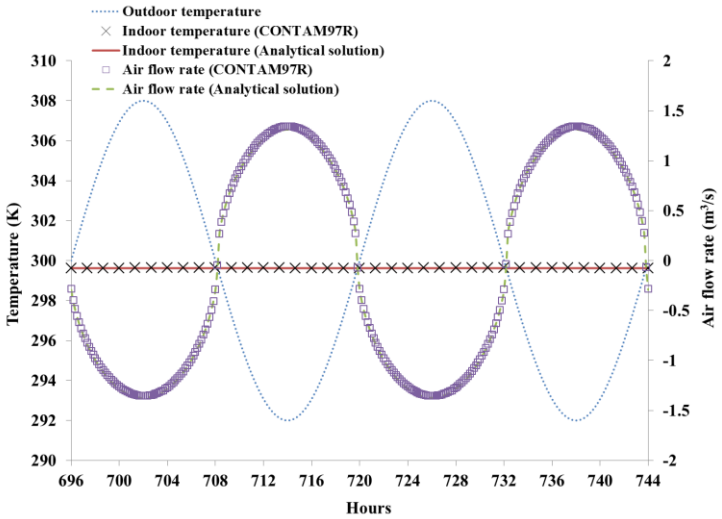

Figure 2: Comparison between the simulation and the analytical solutions in the natural ventilation in a single-zone room.

4 Smoke dispersion in a high-rise building

Analytical model

Another group of flows induced by stack effect is the movement of hot gas in buildings, such as the dispersion of hot smoke in high-rise buildings during fires. Qi et al. (2014) developed an analytical model of the smoke dispersion through high-rise shafts during fires. In this section, we first summarize the analytical model, and then investigate how to use CONTAM97R to model the smoke dispersion, and finally evaluate how the program performs by comparing the simulation results to the analytical solutions.

For the building with a fire located at the first floor in Figure 3, the analytical model can be developed by taking the following assumptions: (1) smoke movement in the shaft is one-dimensional at steady state; (2) the outdoor air temperature and the building temperature at non-fire floors are constant; (3) specific heat capacity of the smoke, C_p, is constant; (4) the smoke is assumed to be incompressible and viscous but thermally expansible satisfying the ideal gas law; (5) no smoke leaks through shaft walls; (6) heat transfer coefficients (either due to convection or radiation) are constant and do not vary along the height of the shaft; (7) the temperature of the fire floor is uniform and maintained at the fire smoke temperature.

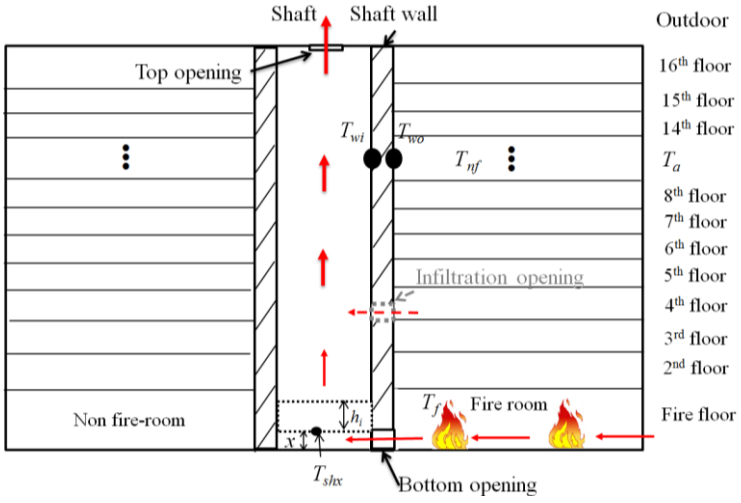

Figure 3: Schematic of a building driven by stack effect

Eqs. (11) ~ (23) show the formulations for the temperature profiles (including the smoke temperature in the shaft, the interior and exterior wall temperature of the shaft), the pressure profile and the smoke flow rate, which are derived from the heat balance equation, mechanical energy equation and mass balance equation, respectively. The fire room pressure, p_f, in Eq. (20) can be obtained from Eq. (23). The neutral pressure level of the fire room is assumed at the middle height as suggested by Tamura (1994).

- Temperatures of smoke, interior and exterior shaft walls

$$T_{shx} = T_b + (T_f - T_{nf})Exp(-\alpha x / H) \tag{11}$$

$$T_{wix} = T_{nf} + (T_f - T_{nf})(1 - 1/(h_{wi}R_t))Exp(-\alpha x / H) \tag{12}$$

$$T_{wox} = (T_{wox} - T_{nf})/(T_f - T_{nf}) = (T_f - T_{nf})Exp(-\alpha x / H)/(h_{wo}R_t) \tag{13}$$

where

$$\alpha = PH/(\dot{m}C_p R_t) \tag{14}$$

$$R_t = 1/h_{wi} + W/\lambda + 1/h_{wo} \tag{15}$$

- Pressure profile

$$p_{shx} = p_{sh0} - \Delta p_{dyx} - \Delta p_{elx} - \Delta p_{frx} \tag{16}$$

where:

$$\Delta p_{dyx} = \frac{\dot{m}^2 R(T_f - T_{nf})}{p_{a0}A_h^{\ 2}}[Exp(-\alpha x / H) - 1] \tag{17}$$

$$\Delta p_{elx} = \frac{g p_{a0} H}{R T_{nf}} \left\{ \frac{1}{\alpha} \ln \left[\frac{(T_f - T_{nf}) + T_{nf} EXP\left(\frac{Px}{\dot{m}C_p R_t} \right)}{T_f} \right] \right\} \tag{18}$$

$$\Delta p_{frx} = \frac{f\dot{m}^2 R H T_{nf}}{2D_h A_h^{\ 2} p_{a0}} \left\{ \frac{x}{H} + \frac{1}{\alpha} \frac{T_f - T_{nf}}{T_{nf}} \left[1 - EXP\left(\frac{-xP}{\dot{m}C_p R_t} \right) \right] \right\} \tag{19}$$

- Smoke mass flow rate

$$\dot{m}_b = C_d A_b \sqrt{2(p_f - p_{sh0}) p_{a0}/(RT_f)} \tag{20}$$

$$\dot{m}_t = \dot{m}_b = C_d A_t \sqrt{2(p_{shH} - p_{aH}) p_{a0}/(RT_{shH})} \tag{21}$$

where

$$p_{sh0} = p_f - \dot{m}_b^{\ 2}/[(C_d A_b)^2 (2\rho_f)] \tag{22}$$

$$p_f = p_a - \Delta p_f = p_a - g(x - x_{npl})\rho_a (T_f - T_a)/T_f \tag{23}$$

The above equations show that the smoke flow through the shaft is closely coupled with the heat transfer between the smoke and the surroundings. To solve the above equations, an iterative procedure is introduced following, which just needs simple hand calculation instead of solving complex matrixes of discretized equations, and avoids potential errors due to numerical discretization (Qi et al. 2014) .

Given the superscript indicates the current iteration:

(i) Get R_t, and p_f by Eqs. (15) and (23) respectively.

(ii) Get $\alpha^{(1)}$ by estimating smoke mass flow rate $\dot{m}_b^{(1)}$, and calculate $\alpha^{(1)}$ by Eq. (14).

(iii) Get $p_{shH}^{(1)}$ by calculating $p_{sh0}^{(1)}$ using Eq. (22), calculate $\Delta p_{dyx}^{(1)}$, $\Delta p_{elx}^{(1)}$and $\Delta p_{frx}^{(1)}$ by Eqs. (17)~(19), and then calculate $p_{shH}^{(1)}$ by Eq. (16) when $x = H$.

(iv) Get $\dot{m}_t^{(1)}$ by calculating $T_{shH}^{(1)}$ using Eq. (11), and calculate $\dot{m}_t^{(1)}$ by Eq. (21).

(v) If $|\dot{m}_t^{(1)}-\dot{m}_b^{(1)}|/\dot{m}_t^{(1)}$ is over a convergence threshold, let $\dot{m}_b^{(2)}= (\dot{m}_t^{(1)}+\dot{m}_b^{(1)})/2$, and then return to steps (ii) – (v) till the convergence is reached.

(vi) Obtain α, T_{sh}, T_{wi}, T_{wo} and p_{shx} using Eqs. (14), (11), (12), (13) and (17), respectively.

Simulation setup

Based on the building schematic in Figure 3, the modeled building in this study is chosen as a 16-floor high-rise (see Table 2). The shaft can be considered as an elevator shaft without any elevator car, because the current analytical solution cannot consider the case with the car. Here, the shaft is considered well sealed (no smoke infiltration to non-fire floors) with only one opening at each end of the shaft as shown in Figure 3. Four cases of the leakage levels for the top and bottom openings are based on different opening areas as Table 2 shows. A fire characterized by a fire temperature of 975.15 K is located at the first floor (the fire floor), representing one of the worst fire scenarios. During the fire, the fire smoke would enter the shaft and spread across all higher floors. Since the analytical solutions are at the steady state, we run the transient simulation enough time to reach the results at the steady state, confirmed by checking the time-variant temperature in the shaft is less than a threshold value of 1×10^{-4} K.

Table 2：Simulation set-up in CONTAM97R

List of conditions	Value
A. Building conditions	
Number of floor	16
Height First floor	8 m
Height of other floor (2^{nd}~15^{th} floor)	4 m
Non-fire floor temperature	293.15 K
B. Shaft conditions	
Height	68 m
Roughness	0.1 m [a]
Cross section	5 m × 12 m
shaft wall width	0.24 m
Bottom and top opening area	0.1 m^2 (Case 1), 0.2 m^2 (Case 2), 0.5 m^2 (Case 3), 1.0 m^2 (Case 4)
Discharge coefficient	0.6
Material of shaft	Concrete
Conduction heat transfer coefficient	1.7 W/ (m·K) [b]
Heat transfer coefficient	10 W/ (m^2·K)
C. Fire conditions	
Fire room Temperature	975.15 K
D. Atmospheric conditions	
Outdoor temperature	253.15 K

Outdoor pressure at the level of ground	101325 Pa

[a] Roughness of shaft is selected from Klote et al. 2012.

[b] Conduction heat transfer coefficient is selected from Guo et al. 2011.

A building space is defined in CONTAM97R as a zone with a uniform temperature. The shaft is characterized as a vertical and long building space, which can be divided by different strategies. As a result, the zoning strategies directly affect the simulated temperature distribution in the shaft, and consequently the simulated shaft pressure profile and the smoke flow rate, which are closely coupled to the temperature prediction. A poor zoning strategy could cause significant simulation errors, which should not be attributed to a failure of CONTAM97R. The verification study in the following sections identifies such situations and suggests a better zoning strategy to improve the simulation efficiency.

Floor Zoning Strategy (FZS)

One of the most common methods of dividing the shaft is probably to assign one zone for each floor or to further divide each floor zone into several sub-zones with equal size (Klote et al. 2012, Miller 2011). For this so-called "Floor Zoning Strategy" (FZS), we first studied the case of one zone assigned for each floor, which resulted in a total of 16 zones for the modeled high-rise building.

Figure 4 and Table 3 compare the predicted temperature and pressure profiles, and mass flow rate by CONTAM97R to the analytical solutions for all the four cases with different opening sizes (see Table 2). It was found that the predicted temperature error of exterior shaft wall is smallest (11%) (Figure 4(c)), while that of the smoke in the shaft is largest (27%) (Figure 4(a)). This is because the smoke is farthest from, while the exterior shat wall is nearest to, the air in the non-fire floor, which is known and set as the boundary condition in the simulation. Figure 4 and Table 3 also indicate that a larger value of α will lead to worse predicted results (includes temperatures, pressure and smoke flow rate) by CONTAM97R, and the value of α has more influence on the simulation accuracy of temperature than on the simulation accuracy of pressure and smoke flow rate. For a specific case, the value of α is inversely proportional to the value of smoke flow rate according to Eq. (14). A large α (e.g. α = 11.56), means small smoke flow rate and quick dropping of the smoke temperature at the entrance of the shaft (0~16m in this case). Therefore, zoning with equal size for each floor cannot resolve the temperature gradient at the lower floors. Since the smoke pressure and flow rate are related to the smoke temperature, the error of predicted temperature also results in errors of predicted pressure and smoke flow rate.

The simulations also revealed some key information on the risk assessment of the smoke movement from the fire floor to the higher floors. In Figure 4 (d), as the opening area increases (e.g. from Case 1 to Case 4), the neutral pressure level (NPL) decreases, and the pressure difference between the shaft and non-fire floor increases, indicating more non-fire floors will be potentially exposed to smoke. Therefore, the opening size in a high-rise shaft should be carefully designed for the concerns of fire smoke safety.

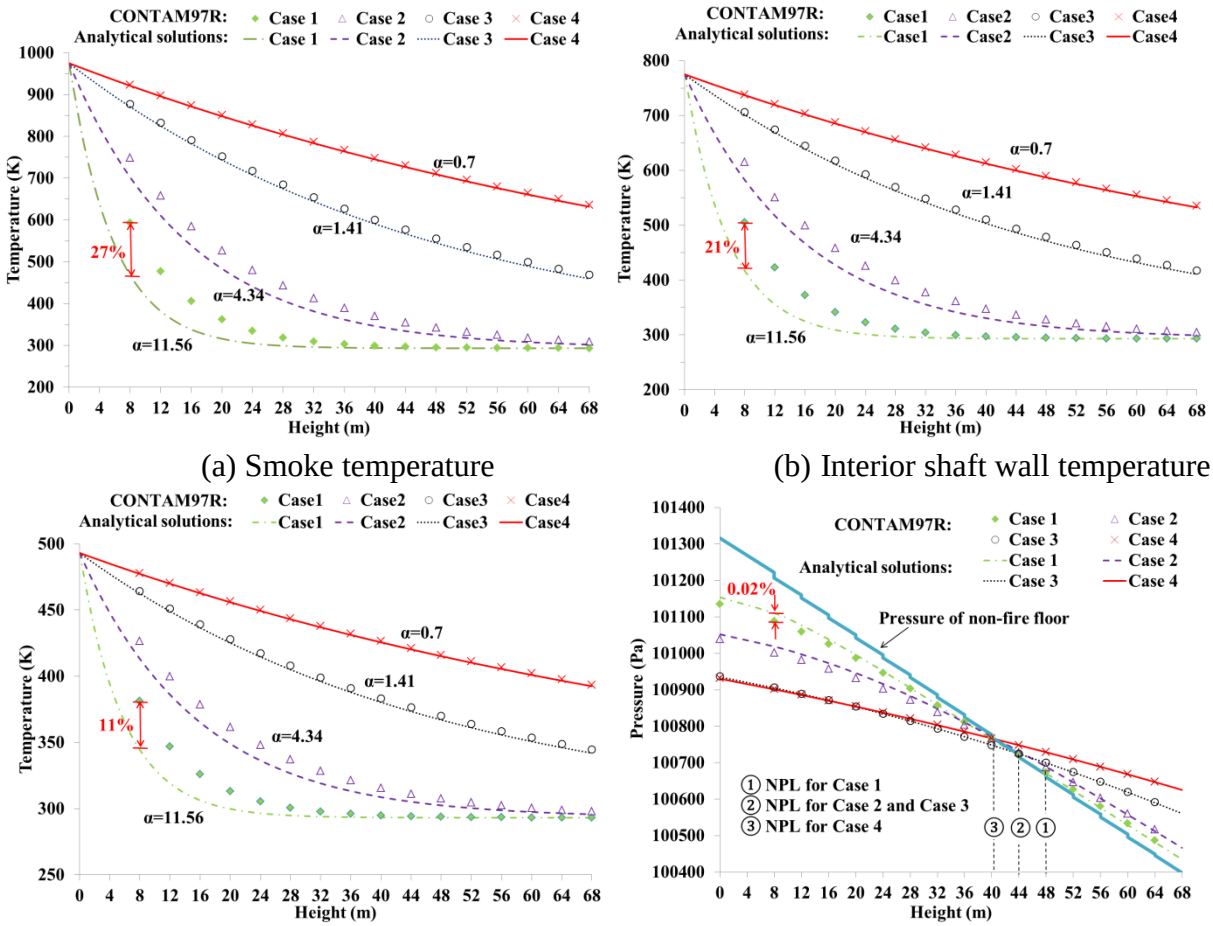

(a) Smoke temperature

(b) Interior shaft wall temperature

(c) Exterior shaft wall temperature

(d) Pressure

Figure 4: Comparison between results of CONTAM97R and analytical solutions for different cases with FZS (total zones = 16)

Table 3：Mass flow rate (kg/s) of CONTAM97R and analytical solutions

	Case 1 (α=11.56)	Case 2 (α=4.34)	Case 3 (α=1.41)	Case 4 (α=0.7)
CONTAM97R mass flow rate	0.624	1.597	4.753	9.580
Analytical solutions of mass flow rate	0.584	1.556	4.772	9.611
Errors (%)	6.8%	2.6%	0.4%	0.3%

Considering that 16 zones are not sufficient to achieve accurate results for cases with high α, we divided each floor into more sub-zones with equal size. The zone-heights are reduced to 2m (total zones = 34), 1m (total zones = 68) and 0.5m (total zones = 136). The temperature profiles and mass flow rate are plotted in Figure 5(a) and Figure 5(b). The results show that as the number of total zones increases, the simulation results are closer to the analytical solutions. Meanwhile, the accuracy cannot be further improved when the total zones change from 68 to 136. It shows that the results no longer depend on the refined zones: there seems to exist zone-independent results in this case.

Although creating more zones using FZS can achieve zone independent results, it is not an efficient zoning strategy. In Figure 5 (a), it can be observed that the temperature gradient varies significantly along the shaft height: most of the temperature change occurs at the height of 0~16m. Using an equal number of sub-zones for each floor, FZS tends to create

many unnecessary zones where there is a small temperature gradient. Therefore, a better zoning strategy would be to create sub-zones adaptively based on temperature gradients.

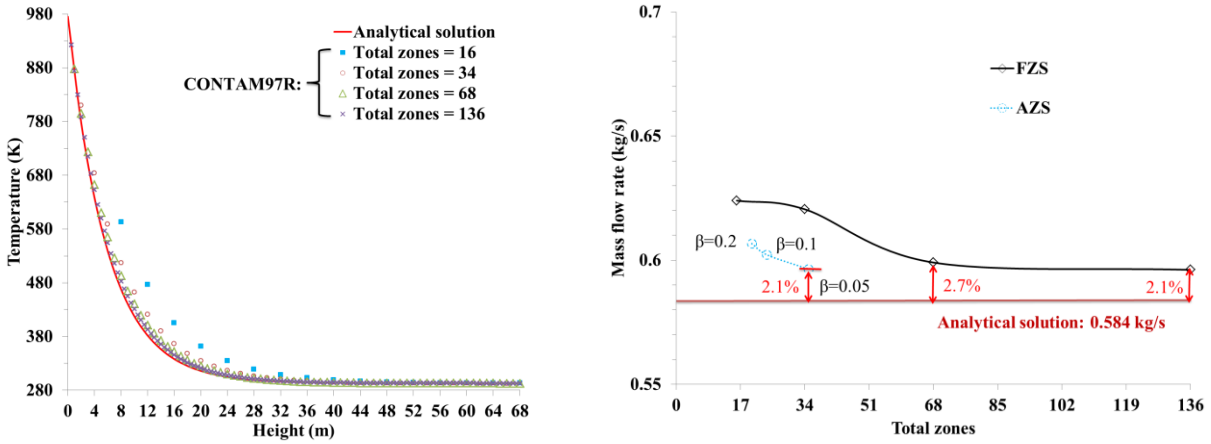

(a) Temperature (FZS) (b) Mass flow rate

Figure 5: Effects of total zones number on the CONTAM97R results (Case 1)

Adaptive Zoning Strategy (AZS)

To create adaptive zones based on temperature gradient, we proposed a new zoning method, named Adaptive Zoning Strategy (AZS), which limits temperature difference between two neighboring zones by a temperature constraint, β as Eq. (24) shows. θ_{shx} is the dimensionless smoke temperature in the shaft of Figure 3, derived by Qi et al. (2014). So the height of each zone, h_i, can be obtained (see Eq. (26)).

$$\beta = \theta_{shx} - \theta_{sh(x+h_i)} \qquad (0<\beta<1) \tag{24}$$

where

$$\theta_{shx} = \left(T_{shx} - T_{nf}\right)/\left(T_f - T_{nf}\right) = Exp\left(-\alpha x / H\right) \tag{25}$$

$$h_i = H \ln\left[1 - \beta Exp\left(x\alpha / H\right)\right]/\left(-\alpha\right) \tag{26}$$

In CONTAM97R, each floor of the shaft must contain at least one zone, and each zone cannot cross two floors, which was considered when AZS is used to create zones here. Zone size and simulation results of AZS and FZS of Case 1 are listed in Figure 5(b), Figure 6 and Figure 7, which show that AZS can improve simulation accuracy greatly with fewer zones. For example, the AZS with β=0.05 only needs 35 zones, which is one fourth of FZS (total zones = 136), to reach results with similar accuracies for the mass flow rate (Figure 5(b)) and the predicted temperature (Figure 7). Therefore, AZS is more efficient in terms of zone numbers and predicted accuracy for the multi-zone airflow and energy network model.

It can also be found that for a specific value of α, the predicted accuracy of AZS is determined by β. When a smaller β is chosen, more zones will be created and the simulation results will be better. Moreover, once β is chosen, zones numbers and height of each zone are determined, for which the associated simulation accuracy is then determined (e.g. the largest error of temperature is 4.4% for β=0.05 in this case). Therefore the accuracy of AZS simulation could be obtained if α and β are known. This feature of AZS is helpful to obtain the results with known accuracy.

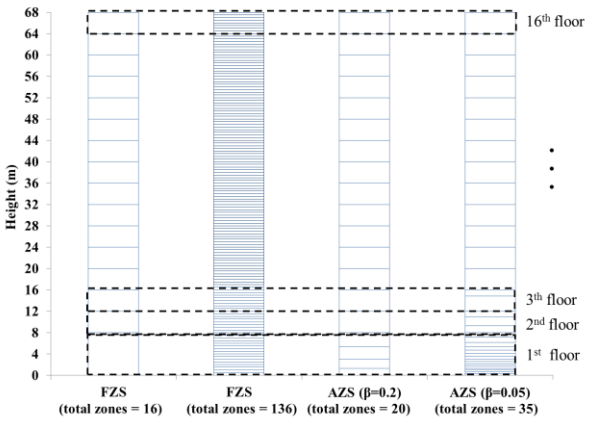

Figure 6: Zone heights for different zoning strategies (Case 1)

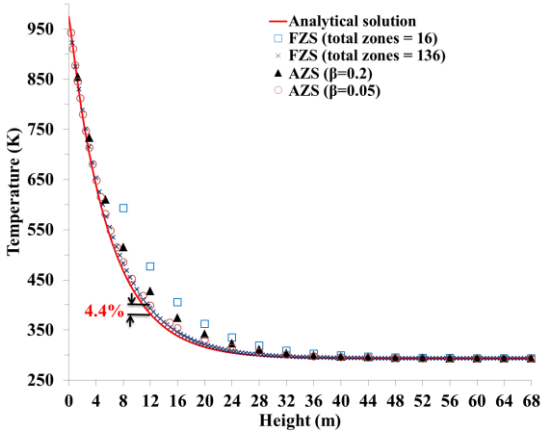

Figure 7: Comparison of temperature profile between analytical solution and different zoning strategies (Case 1)

5 Conclusion

This study verified a multizone airflow and energy network model (CONTAM97R) using the analytical solutions to airflows induced by stack effect in a single-zone room and smoke flows in the air-tight high-rise shaft during fires. Two zoning methods to divide the shaft into multiple sub-zones, FZS and AZS, were proposed and compared. The study reached the following major conclusions:

- Accurate results can be obtained by COMTAM97R for the natural ventilation in a single-zone room.

In the study of the smoke dispersion in a high-rise building:

- when zones are chosen appropriately, COMTAM97R can obtain accurate results.
- simulation errors of FZS are related to the temperature attenuation coefficient, α. The larger α, the bigger the errors will be.
- there seems to exist zone-independence results. For the case study of FZS in this paper, when total zones is more than 68 (zone height = 1m), the results will not be further improved by the increase of zones.
- by comparing simulation results of FZS and AZS, AZS is found to be more efficient. AZS can contribute to more accurate results with fewer zones.
- the examples in this paper reveal that the increasing opening area at the entrance and top of the shaft will result in more floors exposed to fire smoke.

It should be noted that although this study is based on CONTAM97R, the analytical solutions and the proposed zoning strategies can be applicable to other similar multizone airflow and energy network models.

Nomenclature

A	opening area
B	buoyancy flux
C_d	discharge coefficient
C_p	specific heat capacity of the air
D_h	hydraulic diameter
E	heat source

F	volume flow rate
h	heat transfer coefficient; height
k	thermal conductivity
m	mass of thermal mass
$\dot{m}$	mass flow rate
p	pressure
P	perimeter of the shaft
q	heat flux
R	specific gas constant
R_t	thermal resistance between two sides of the shaft
t	time
T	temperature
$\tilde{T}$	average temperature
W	thickness of the shaft wall
x	height of interests

Greek symbols

α	temperature attenuation coefficient
β	temperature constraint
Δ	difference
η	buoyancy air change parameter
θ	normalized temperature
λ	outdoor temperature fluctuation air change parameter
ρ	density
φ	thermal mass number
ω	frequency of outdoor temperature variation

Subscripts

0	ground level, the height of $x = 0$
a	atmospheric
b	bottom
dy	dynamic
el	elevation in the shaft
f	fire floor
fr	friction
H	height of the shaft
i	zone symbol; interior shaft wall
j	zone symbol
n	zone number
nf	non-fire floor
npl	neutral plane level

o	outdoor; exterior shaft wall
t	top
sh	shaft
w	wall

6 Acknowledgements

The authors acknowledge the financial supports from the Discovery Grants of the Natural Sciences and Engineering Research Council of Canada (NSERC), the Graduate Student Support Program (GSSP), and the 2013 SEED Individual Funding of the Faculty of Engineering and Computer Science of Concordia University.

7 References

Axley, J.W, 2011. Application of natural ventilation for U.S. commercial buildings, Report, GCR-01-820, National Institute of Standards and Technology, Gaithersburg, MA.

Axley, J.W., Emmerich, S.J., Walton, G.N., 2002. Modeling the performance of a naturally ventilated commercial building with a multizone coupled thermal/airflow simulation tool, ASHRAE Transactions, 108(2): 1-15.

Chen, Q., 2009. Ventilation performance prediction for buildings: A method overview and recent applications, Building and Environment, 44 (4): 848-858.

Gu, L., 2011. Advanced of EnergyPlus and its coupling with CHAMPS-whole building, Proceedings of CHAMPS 2011: The 8th International Forum and Workshop on Combined Heat, Air, Moisture and Pollutant Simulations, Nanjing, China.

Guo, L.X., Guo, L., Zhong, L., Zhu, Y.M., 2011. Thermal conductivity and heat transfer coefficient of concrete, Journal of Wuhan University of Technology-Mater. Sci. Ed., 26 (4): 791-796.

Haghighat, F., Li, H., 2004. Building airflow movement—validation of three airflow models. Journal of Architectural and Planning Research, 21(4): 331–49.

Klote, J.H., Milke, J.A., Turnbull, P.G., Kashef, A., Ferreira, M.J., 2012. Handbook of Smoke Control Engineering, American Society of Heating, Refrigerating and Air-Conditioning Engineers, Inc., Atlanta.

Miller, R.S., 2011. Elevator shaft pressurization for smoke control in tall buildings: The Seattle approach, Building and Environment, 46(11): 2247-2254.

Miller, R.S., Beasley, D., 2009. On stairwell and elevator shaft pressurization for smoke control in tall buildings, Building and Environment, 44(6): 1306-1317.

McDowell, T.P., Emmerich, S., Thornton, J.W., Walton, G., 2003. Integration of airflow and energy simulation using CONTAM and TRNSYS, ASHRAE Transactions, 109(2): 757-770.

McDermott, R., McGrattan, K., Hostikka, S., Floyed, J., 2010. Fire Dynamics Simulator (Version 5) Technical Reference Guide, Volume 2: Verification. National Institute of Standards and Technology, Gaithersburg.

Mahdavi, A, Proglhof, C. 2008. A model-based approach to natural ventilation. Building and Environment, 43(4): 620-627.

Miller, R.S., 2011. Elevator shaft pressurization for smoke control in tall buildings: The Seattle approach, Building and Environment, 46 (11): 2247-2254.

Munson, B.R., Young, D.F., Okiishi, T.H., Huebsch, W.W., 2005. Fundamentals of Fluid Mechanics, sixth ed., John Wiley & Sons, Inc.

Ng, L.C., Musser, A., Persily, A.K., Emmerich, S. J., 2012. Airflow and Indoor Air Quality Models of DOE Reference Commercial Buildings, NIST Technical Note 1734, National Institute of Standards and Technology, Gaithersburg.

Ng, L.C., Musser, A., Persily, A.K., Emmerich, S. J., 2012. Indoor air quality analyses of commercial reference buildings, Building and Environment, 58: 179-187.

Ng, L.C., Musser, A., Persily, A.K., Emmerich, S. J., 2013. Multizone airflow models for calculating infiltration rates in commercial reference buildings, Building and Environment, 58:11-18.

Oberkampf, W.L., Trucano, T.G., 2002, Verification and validation in computational fluid dynamics, Progress in Aerospace Science, 38 (3): 209-272.

Qi, D.H., Wang, L.Z., Zmeureanu, R., 2014, An analytical model of heat and mass transfer through high-rise shafts during fires, International Journal of Heat and Mass Transfer, 72: 585-594.

Tamura, G.T., 1994. Smoke Movement & Control in High-rise Buildings, National Fire Protection Association, Quincy, MA.

Tan, G., 2005. Study of natural ventilation design by integrating the multi-zone model with CFD simulation, Massachusetts Institute of Technology, Cambridge, MA (Ph.D. thesis)

Tan, G., Glicksman, L.R., 2005. Application of integrating multi-zone model with CFD simulation to natural ventilation prediction, Energy and Building, 37(10): 1049-1057.

Wang, L.Z., Black, W.Z., Zhao, G.C., 2013. Comparison of simulation programs for airflow and smoke movement during high-rise fires, in: ASHRAE 2013 Annual Conference, Denver, CO.

Wang, L.Z., Chen, Q., 2008. Evaluation of some assumptions used in multizone airflow network models, Building and Environment, 43(10): 1671-1677.

Wang, L.Z., Dols, W.S., Emmerich, S.J., 2012. Simultaneous solutions of coupled thermal airflow problem for natural ventilation in buildings, HVAC&R Research, 18(1-2): 264-274.

Yam, J., Li, Y.G., Zheng, Z.H., 2003. Nonlinear coupling between thermal mass and natural ventilation in buildings, International Journal of Heat and Mass Transfer, 46 (7): 1251-1246.